Taylor & Francis
Taylor & Francis Group

Xenobiotica
the fate of foreign compounds in biological systems

ISSN: 0049-8254 (Print) 1366-5928 (Online) Journal homepage: https://www.tandfonline.com/loi/ixen20

Population pharmacokinetic (PK) analysis of laromustine, an emerging alkylating agent, in cancer patients

Ala F. Nassar, Adam V. Wisnewski & Ivan King

To cite this article: Ala F. Nassar, Adam V. Wisnewski & Ivan King (2017) Population pharmacokinetic (PK) analysis of laromustine, an emerging alkylating agent, in cancer patients, Xenobiotica, 47:5, 394-407, DOI: 10.1080/00498254.2016.1201703

To link to this article: https://doi.org/10.1080/00498254.2016.1201703

http://tandfonline.com/ixen
ISSN: 0049-8254 (print), 1366-5928 (electronic)

Xenobiotica

Xenobiotica, 2017; 47(5): 394–407
 DOI: 10.1080/00498254.2016.1201703

Taylor & Francis
Taylor & Francis Group

RESEARCH ARTICLE

Population pharmacokinetic (PK) analysis of laromustine, an emerging alkylating agent, in cancer patients

Ala F. Nassar[1,2], Adam V. Wisnewski[1], and Ivan King[3]

[1]School of Medicine, Department of Internal Medicine, Yale University, New Haven, CT, USA, [2]Department of Chemistry, University of Connecticut, Storrs, CT, USA, and [3]Metastagen Inc, Wilmington, DE, USA

Abstract

1. Alkylating agents are capable of introducing an alkyl group into nucleophilic sites on DNA or RNA through covalent bond. Laromustine is an active member of a relatively new class of sulfonylhydrazine prodrugs under development as antineoplastic alkylating agents, and displays significant single-agent activity.
2. This is the first report of the population pharmacokinetic analysis of laromustine, 106 patients, 66 with hematologic malignancies and 40 with solid tumors, participated in five clinical trials worldwide. Of these, 104 patients were included in the final NONMEM analysis.
3. The population estimates for total clearance (CL) and volume of distribution of the central compartment (V_1) were 96.3 L/h and 45.9 L, associated with high inter-patient variability of 52.9% and 79.8% and inter-occasion variability of 26.7% and 49.3%, respectively. The population estimates for Q and V_2 were 73.2 L/h and 29.9 L, and inter-patient variability in V_2 was 63.1%, respectively.
4. The estimate of V_{ss} (75.8 L) exceeds total body water, indicating that laromustine is distributed to tissues. The half-life is short, less than 1 h, reflecting rapid clearance. Population PK analysis showed laromustine pharmacokinetics to be independent of dose and organ function with no effect on subsequent dosing cycles.

Keywords

Acute myelogenous leukemia, alkylating agent, cancer patients, solid tumors, VNP40101M (Cloretazine)

History

Received 2 May 2016
Revised 9 June 2016
Accepted 11 June 2016
Published online 13 July 2016

Introduction

The sulfonylhydrazines are a new family of potent alkylating agents, from which laromustine (1,2-bis(methylsulfonyl)-1-(2-chloroethyl)-2-[(2-methylamino)carbonyl]) hydrazine, also known as VNP40101M, was selected for clinical development (Penketh et al., 1994; Pratviel et al., 1989; Shyam et al., 1985, 1986, 1987, 1996). The chemical structures of laromustine and its active metabolite VNP4090CE are shown in Figure 1(a). Laromustine decomposition yields nitrogen and chlorine-centered cationic chloroethylating species and methyl isocyanate as shown in Figure 1(b). Alkylation occurs preferentially at the O^6 position in guanine (Penketh et al., 2000). In addition, laromustine has low reactivity with glutathione and glutathione transferase, critical components in the cellular defense against oxidative damage and xenobiotics (Meister & Anderson, 1983; Moriarty-Craige & Jones, 2004). In murine models, laromustine demonstrated anti-tumor activity against leukemia and solid syngeneic and human xenograft tumors (Finch et al., 2001).

Address for correspondence: Ala F. Nassar, Ph.D., Yale University, School of Medicine, 300 Cedar St/TAC s416, New Haven, CT 06510, USA. Tel: +1 203 809 9608. E-mail: ala.nassar@yale.edu

Laromustine as a single agent was initially studied in three phase I trials. The first of these trials (study CLI-011) included patients with advanced solid tumors treated by intravenous (IV) infusion over 15–30 min at dose levels ranging from 3 to 305 mg/m^2 every 4–6 weeks. The maximum tolerated dose (MTD) was 305 mg/m^2 and the dose-limiting toxicity was reversible myelosuppression. No drug-related dose-limiting non-hematologic toxicities were observed. The second phase I trial (study CLI-028) was also conducted in patients with advanced solid tumors. Patients were given three IV treatments weekly in four-week cycles at first cycle doses of 80, 100, 125 and 155 mg/m^2. The third phase I study (study CLI-029) consisted of patients with relapsed or refractory leukemia given IV treatments at doses ranging from 220 to 708 mg/m^2 with treatment repeated monthly as indicated. A dose level of 600 mg/m^2 was considered well-tolerated, with no observable dose-limiting non-hematologic toxicities, and was selected for phase II evaluation.

A phase II trial of laromustine at a dose of 600 mg/m^2 was conducted in two strata of patients with hematologic malignancies (study CLI-033). Patients 60 years or older (median age 72, range 60–84) with poor-risk acute myelogenous leukemia (AML), including both *de novo* and secondary AML, or patients with high-risk myelodysplastic

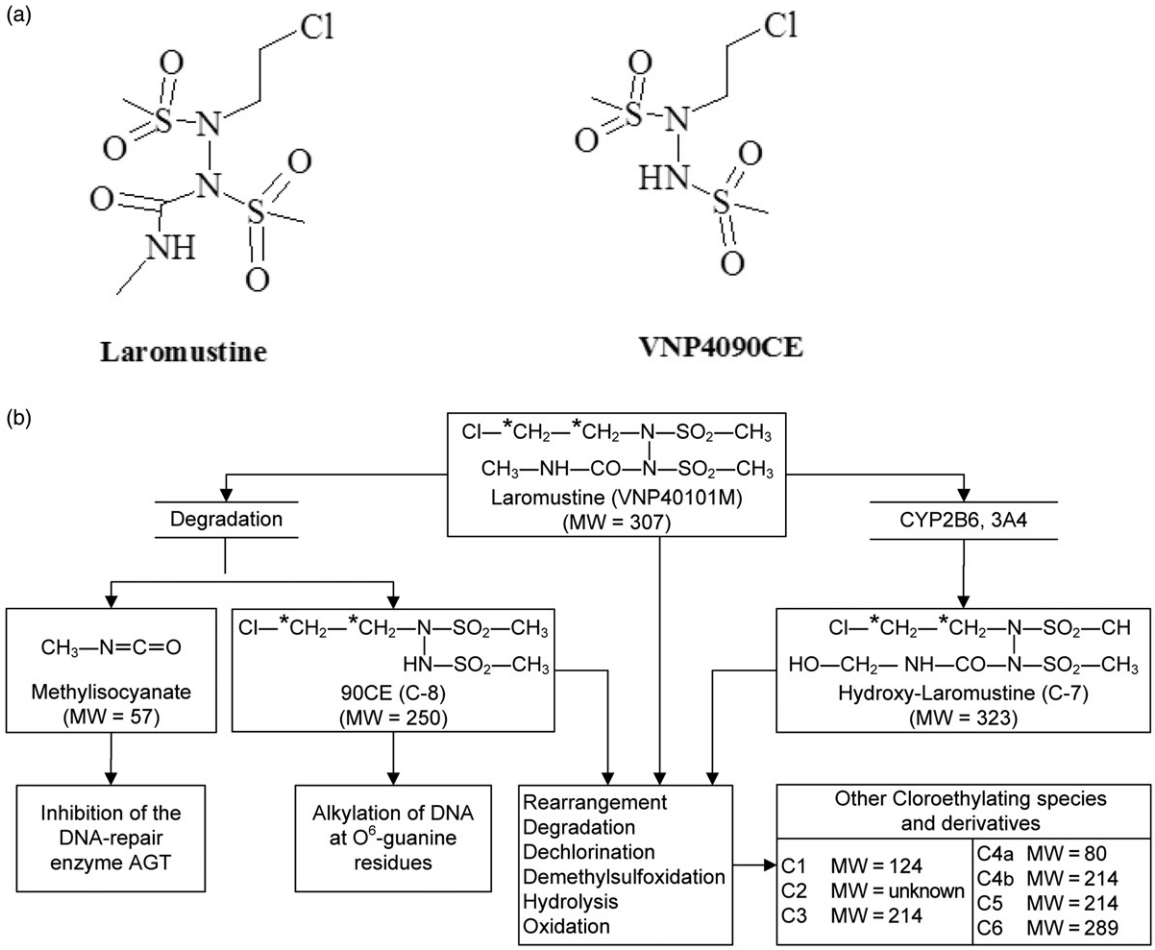

Figure 1. (a) Chemical structures of laromustine and VNP4090CE. (b) Chemical structure of laromustine and its metabolite/degradation products (from Nassar et al., 2009).

syndrome (MDS) were treated in Stratum A. Patients with AML in first relapse (median age 62, range 18–84 years) were treated in Stratum B. The overall response rate (ORR) including both CR and CR with incomplete platelet recovery (CRp) indicated that the drug was active with an early death rate consistent with that of other agents approved in this indication. Patients 60 years or older with *de novo* poor-risk acute myelogenous leukemia (AML) or high-risk MDS had a better ORR than patients with secondary AML or AML in first relapse.

Given the encouraging level of activity in *de novo* AML, a phase II trial of laromustine at a dose of 600 mg/m^2 was conducted in patients 60 years or older with *de novo* poor-risk AML (study CLI-043). A second induction cycle was administered at the same dose 4–5 weeks after the first cycle if the bone marrow was improved but contained residual disease. For patients achieving CR or CRp after the first or second induction cycle, or partial response (PR) after a second induction cycle, one or two consolidation cycles of AraC continuous infusion at a dose of 400 mg/m^2/day for 5 days could be administered, starting 45–90 days after the last induction cycle. PK data were collected from the phase I dose escalation trials in patients with solid tumors (studies CLI-011 and CLI-028), and hematologic malignancies (study CLI-029). PK assessments were also performed in a cohort of patients with AML or high-risk MDS in the phase II trials CLI-033 and CLI-043. These data have been previously analyzed for each study separately (Abdelhameed, 2008; Jiang, 2008; Nassar, 2008a,b,c) and the PK parameters estimated are summarized in Table 1.

The geometric mean terminal half-life ($t_{1/2z}$) was consistently less than 1 h in estimates from all studies. High inter-patient variability was observed in all other laromustine PK parameters estimated in the phase I studies. Body surface area normalization of mean systemic plasma clearance (CL) or mean volume of distribution at steady state (V_{ss}) for all patients at all doses of laromustine did not alter this variability. In the phase II studies (CLI-033 and CLI-043), conducted at a first cycle dose of 600 mg/m^2, high inter-patient variability was also observed in these laromustine PK parameters. Overall the CL and V_{ss} estimated from these phase II studies appear somewhat larger than those reported from the phase I studies. However, more than 90% variability is associated with the CL and V_{ss} estimates in the phase II studies. The mean CL value ranged from 95.0 to 352 L/h across the studies (48.0–181 L/h/m^2 when normalized for body surface area). Similarly, V_{ss} ranged from 60.4 to 370 L (31.1–192 L/m^2 when normalized for body surface area). These estimates of systemic clearance are greater than the human liver blood flow rate and approximately equal to total cardiac output (Davies & Morris, 1993).

Table 1. Summary of PK parameters from laromustine clinical studies.

		Phase I			Phase II	
PK parameter		CLI-011	CLI-028	CLI-029	CLI-033	CLI-043
CL (L/h)	Mean ± SD	95.0 ± 70.7	272 ± 190	103.1 ± 71.9	352 ± 353	261 ± 529
	CV (%)	74	70	70	100	203
AN CL (L/h/m^2)	Mean ± SD	48.0 ± 31.1	143 ± 98	54.3 ± 38.8	181 ± 172	125 ± 229
	CV (%)	65	68	71	96	183
V_{ss} (L)	Mean ± SD	60.4 ± 23.3	206 ± 146	89.6 ± 64.4	370 ± 339	321 ± 636
	CV (%)	39	71	72	92	198
AN V_{ss} (L/m^2)	Mean ± SD	31.1 ± 10.0	107 ± 72	46.5 ± 32.5	192 ± 168	154 ± 277
	CV (%)	32	67	70	87	179
$t_{1/2z}$ (h)	Mean ± SD	0.673 ± 0.204	0.677 ± 0.160	0.699 ± 0.238	0.695 ± 0.169	0.841 ± 0.155
	CV (%)	30	24	34	24	18

AN = normalized for body surface area.

The very high CL is consistent with extra-hepatic elimination. The rapid, non-enzymatic degradation characteristic of laromustine is also consistent with this high clearance rate. The estimate of V_{ss} exceeds total body water for humans (Davies & Morris, 1993), indicating that laromustine is distributed extensively in tissues.

Population PK modeling aims to explain variability by identifying factors of demographic or pathophysiological origin that may influence the PK behavior of a drug and to provide quantitative estimation of the magnitude of the unexplained variability in the patient population. In mixed-effects modelling, this is achieved by estimating population mean parameter values (derived from fixed-effects parameters) and their variability within the population (derived from random-effects parameters) directly from the full set of individual data. The population PK approach offers the possibility of gaining integrated information on the PK of drugs from relatively sparse data or a combination of sparse and dense data, and allows pooled analysis of data from a variety of unbalanced study designs that is characteristic of most cancer patient studies.

Recently, we published the results of several *in vitro* and *in vivo* studies that were designed to examine the biotransformation and rearrangement of laromustine. High mass accuracy and ultrahigh resolution measurements, H-D, stable-isotope labeled analogue (^{13}C-labeled laromustine), NMR, and detailed analyses of the LC–MS^n experiments were used to assist with the assignments of these fragments and possible mechanistic rearrangement. The results showed that laromustine undergoes rearrangement, dehalogenation and hydrolysis at physiological pH to form active moieties. Laromustine produces several reactive metabolites which were trapped by glutathione (GSH), *N*-acetylecysteine (NAC) and cysteine (CYS) in the *in vitro* systems (Nassar et al., 2009, 2010a,b,c, 2011, 2015). Herein we report for the first time the details of the methodology and results of the population PK analysis of laromustine using mixed-effects modeling and the combined data obtained in the phase I studies CLI-011, CLI-028 and CLI-029 and phase II studies CLI-033 and CLI-043.

Methods

Data

Laromustine plasma concentration–time profiles were available from five clinical trials in cancer patients, conducted by Vion Pharmaceuticals, Inc. (Vion, New Haven, CT). Studies CLI-011 and CLI-028 were phase I dose escalation studies in patients with solid tumors. Study CLI-029 was a phase I dose escalation study conducted in patients with hematologic malignancies. PK assessments were also performed in a cohort of patients with AML or high-risk MDS treated with the MTD in the phase II study CLI-033. Additional PK samples were collected in AML patients treated in the confirmatory phase II study CLI-043.

Laromustine injection

It was supplied in 10 mL clear glass vials for all studies. The first lot manufactured, Lot 00-07-0027, contained 100 mg of laromustine formulated in a solution consisting of 30% (3 mL) anhydrous ethyl alcohol, USP and 70% (7 mL) polyethylene glycol 300, NF, and was diluted with 5% dextrose for injection, USP prior to infusion. This Lot was used to treat the first three patients in study CLI-011 only. For all subsequent lots, the formulation was slightly modified to include citric acid. The new formulation used in all studies contained 100 mg of laromustine formulated in a solution consisting of 30% (3 mL) anhydrous ethyl alcohol, USP, 70% (7 mL) polyethylene glycol 300, NF, with 0.6% (6 mg/mL) anhydrous citric acid, USP, and was diluted with 5% dextrose for injection USP prior to infusion.

Bioanalytical methods

Concentrations of laromustine in human plasma were determined by three different validated analytical methods using high performance liquid chromatography (HPLC) with tandem mass spectrometric (MS/MS) detection (18, 19, 20). The concentration ranges and the lower limit of quantitation (LLOQ) for each method used in each study are shown below. Concentrations below the respective LLOQ were excluded from the NONMEM dataset.

Bioanalytical methods used to measure plasma concentration of laromustine:

Study	Method	Lab	LLOQ	Assay range
CLI-011	QC-T035	Vion	26 ng/mL	26–2600 ng/mL
CLI-028	MET010	NEBA	10 ng/mL	10–5000 ng/mL
CLI-029	MET010	NEBA	10 ng/mL	9–4571 ng/mL
	QC-T035	Vion	26 ng/mL	26–2600 ng/mL
CLI-033	VNPHPP	Covance	1 ng/mL	1–1000 ng/mL
CLI-043	VNPHPP	Covance	1 ng/mL	1–1000 ng/mL

Vion study CLI-011

This was a dose escalating, open label, non-randomized phase I trial in patients with advanced or metastatic cancer (solid tumors). Patients received laromustine IV over 15–30 min at concentrations up to 4 mg/mL. Dose was escalated in successive cohorts of patients with cycles repeated every 4–6 weeks. Twenty-four patients receiving first cycle dosages ranging from 3 to 305 mg/m^2 were included in the PK portion of the study and 16 of the 24 patients had blood collected and PK calculated for more than one cycle. Blood samples for PK analysis were collected at the following time points on day 1 of each of the first two cycles and in any cycle with a change in dose: pre-infusion, at the end of the infusion, and at 5, 10, 20 and 40 min, 1, 2 and 4 h after the end of the infusion.

Vion study CLI-028

This was a dose escalating, open label, non-randomized phase I trial in patients with advanced or metastatic cancer (solid tumors). Patients received laromustine IV over 15 min at concentrations up to 2 mg/mL, with the dose escalated in successive cohorts of patients. Seventeen patients receiving first cycle dosages of 80, 100, 125 and 155 mg/m^2 weekly $\times$ 3 in four-week cycles were included in the PK portion of the study. Ten of the 17 patients received more than one cycle and contributed blood samples for additional PK analyses. Blood samples for PK analysis were collected on day 1 of each of the first two cycles at the following time points: pre-infusion, at the end of the infusion, and at 5, 10, 20 and 40 min, 1, 2 and 4 h after the end of the infusion.

Vion study CLI-029

This was a dose escalating, open label, non-randomized phase I trial in patients with hematologic malignancies. Patients received laromustine IV ranging from 220 to 708 mg/m^2 over 15–30 min for a final dilution volume $\leq$250 mL, over 30–60 min for final dilution volume of 251–500 mL, and over 60–90 min for final dilution volume of 1000 mL. Dosing was administered every four weeks for up to six cycles. Thirty-five patients were included in the PK portion of the study. Among them, 10 patients had PK data collected in more than one cycle. Blood samples for PK analysis were collected at the following time points on day 1 for the first two cycles and in any cycle with a change in dose: pre-infusion, at the end of the infusion, and at 5, 10, 20 and 40 min, 1, 2 and 4 h after the end of the infusion.

Vion study CLI-033

This was an international, open label, phase II, multicenter trial in patients with AML or MDS. Patients received laromustine 600 mg/m^2 IV over 30 min in a total volume of 500 mL. A second cycle was administered at the same dose, 4–5 weeks after the first cycle if the bone marrow was improved but contained residual disease. A consolidation course of laromustine at a reduced dose of 400 mg/m^2 could be administered to patients achieving CR or CRp after the first or second induction cycle. Blood samples for PK analysis were collected for a subgroup of 17 patients at the following time points on day 1 of each cycle: pre-infusion, at the end of the infusion, and at 5, 10, 20 and 40 min, 1, 2 and 4 h after the end of the infusion.

Vion study CLI-043

This was an international, open label, phase II, multicenter trial in patients 60 years or older with *de novo* poor-risk AML. Patients received laromustine 600 mg/m^2 IV over 60 min in a total volume of 500 mL. A second induction cycle was administered at the same dose, 4–5 weeks after the first cycle if the bone marrow was improved but contained residual disease. For patients achieving CR or CRp after the first or second induction cycle, or PR after a second induction cycle, one or two consolidation cycles of AraC continuous infusion at a dose of 400 mg/m^2/day for 5 days could be administered, starting 45–90 days after the last induction cycle. Blood samples for PK analysis were collected for a subgroup of 13 patients at the following time points on day 1 of each cycle: pre-infusion, 30 min after start of the infusion, 5–10 min before the end of the infusion, and at 5, 10, 20 and 40 min, 1, 2 and 4 h after the end of the infusion.

Software

Non-linear mixed-effects modeling was performed using the computer program NONMEM with double precision (version VI), installed on a PC. For data-file construction, data presentation, construction of plots and graphical exploration, WinNonlin™, SAS®, SigmaPlot or the PDx-Pop 2.1 front for NONMEM were used, as appropriate.

Population PK analysis

The population PK (PopPK) data analyses and evaluations were performed according to appropriate guidelines (Guidance for Industry, 1999; Guideline on reporting, 2007) using the mixed-effects approach, as implemented in NONMEM. PopPK data analysis strategy was guided by modeling/statistical selection criteria and consisted of selection of appropriate PK structural models for laromustine, estimation of structural and error model parameters, identification of various covariate (COV) relationships and inter-occasion variability (IOV) and derivation of final empirical Bayesian estimates of individual PK parameters.

Modeling/statistical selection criteria

In general, for a more complex model to be selected, the following criteria were considered collectively:

- Successful convergence of the minimization procedure;
- Termination of the covariance step without warning messages;
- A minimum of three significant digits in the estimated parameters, as a criterion for successful termination of the minimization procedure;
- A statistically significant decrease in the objective function value, as assessed by the log-likelihood ratio, which is approximately χ^2 distributed;
- Standard error of parameter estimates not larger than 50% the parameter value;

- Accuracy in the parameter estimates, as indicated by the 95% CI;
- A correlation coefficient between model parameters <0.95;
- Decrease in residual error estimate (a composite of intra-patient variability, assay variability, errors in clinical procedures, and model misspecification errors);
- A random distribution of the dependent variable (observed laromustine concentrations, OBS) versus population predictions (PRED) across the line of identity;
- A random distribution of OBS versus individual predictions (IPRED) across the line of identity;
- A random distribution in the WRES against PRED and against TIME.

Base model

During development of the base model, the appropriate structural PK model was selected based on visual inspection of exploratory plots, previous experience and model goodness of fit criteria. One, two and three compartment PK structural models were evaluated. Exponential error models were evaluated for inter-patient variability on the structural model parameters.

$$P_i = \theta_i \cdot \exp(\eta_i)$$

where P_i is a PK parameter of the ith individual; θ_i is the mean population estimate; ETA (η_i) is the shift of P_i from θ_i (inter-individual variability; a random variable assumed to be symmetrically distributed around zero with variance–covariance matrix Ω denoted by diagonal elements ($\omega_1^2, \ldots, \omega_m^2$, m being the number of parameters)).

The observations were expressed as follows:

$$\mathrm{OBS}_{ij} = (\theta_i, D_i, t_{ij}) * \varepsilon_{ij}$$

where OBS_{ij} is the jth observation (laromustine plasma concentration) in the ith individual; θ_i is the set of PK parameters for the ith individual; D_i is the administered dose for the ith individual; t_{ij} is the time of collection, after administration, of the jth observation in the ith individual and ε_{ij} is the residual shift of the observation from the model prediction (random variable assumed to be symmetrically distributed around 0 with variance σ^2). Different models for residual variability (additive, proportional and combined error model), representing a composite of deviations due to intra(within)-patient variability, assay variability, errors in clinical procedures, and model misspecification errors, as well as logarithmic transformation of observations and predictions were to be tested.

The first-order conditional estimation (FOCE) or FOCE with interactions (INTER) were to be tested to identify the most appropriate mixed-effects model (Piotmovsky, 2000). If problems were encountered with the above estimation methods, the first-order (FO) method was to be used. To assess whether the difference in the objective function between hierarchical models statistically improved the fit of the model to the data, a decrease in the objective function ($\Delta\mathrm{OFV} \geq 3.84$ ($p < 0.05$, χ^2, 1 df)), when compared to the simpler model was considered significant. The base model consists of the structural PK parameters, inter-patient variability in each parameter and residual variability, without any COVs. Individual empirical Bayes PK parameter estimates were derived.

Covariate model

The base model that best described the data was used for the evaluation of potential COV relationships. Possible COV relationships were first assessed graphically by plotting individual Bayes PK parameter estimates versus COV and then evaluated through population modeling.

In accordance with regulatory guidelines and usual practice with this class of drugs, the effects of the following COVs, as well as IOV, were to be assessed for their significance and clinical relevance on the parameters of the PK structural model:

- Demographics: BSA, age, body weight, gender and ethnic origin;
- Tumor type (hematologic and solid tumors);
- Kidney function, as assessed by creatinine clearance;
- Liver function, as assessed by levels of alkaline phosphatase, ALT, AST, LDH, albumin, total proteins and bilirubin.

Cycle baseline COV values (pre-dose assessments for each cycle) were used for COV testing. In general, the effect of a continuous COV was to be modeled using equations of the following form, centered on the median baseline of each COV:

$$P_i = \theta_i + \theta_{p1} \cdot \left(\frac{\mathrm{COV}}{\mathrm{median}}\right)^{\theta_{p2}}$$

where θ_i is the mean population estimate and θ_{p1} and θ_{p2} are parameters associated with changes in each COV. Reduced forms were also to be tested.

The following models were used to evaluate the effect of dose (DOSE, mg/m^2) on PK parameters:

$$P_i = \theta_i + \theta_{p1} \cdot (\mathrm{DOSE})^{\theta_{p2}}$$

$$P_i = \theta_i + \theta_{p1} \cdot e^{\theta_{p2} \cdot \mathrm{DOSE}}$$

In general, the effect of a categorical covariate (CCOV) was to be modeled as follows:

$$P_i = \theta_i \cdot \left(1 + \theta_{p_1} \cdot \mathrm{CC1}\right) \cdot \left(1 + \theta_{p_2} \cdot \mathrm{CC2}\right)$$

In the above equations θ_i is the mean population estimate for the most common category (coded as 0), θ_{p1} and θ_{p2} are parameters associated with changes in categories 1 and 2 of the COV, respectively, and CC1 and CC2 are fixed to 0 if category equals 0, CC1 and CC2 are fixed to 1 and 0, respectively, if category equals 1, and vice versa if category equals 2.

During COV evaluation, missing COV values were assigned to a separate category. If the total number of patients with a missing COV was 15% or higher, this COV was not to be evaluated in the model, or a sub-population with only complete data was to be used for assessing the effect of the particular COV on a PK parameter.

If feasible, a three stage approach was to be followed:

- In a first step (univariate analysis), the COVs are introduced into the model one at a time. Only the COV

model relationships that are deemed significant, as discussed below, are considered for further COV analysis.

- In a second step (forward selection), the COV that has the highest significance in the model is included first (base 1 model), and the other significant COVs from the first step are then included one by one, in the rank order of their significance. Only COVs resulting in a significant improvement of the fit are retained and this comprises the most complex model (base 2 model).
- In the third step (backward elimination), COVs are removed from the most complex model one at a time in the order of their significance until no further insignificant COVs remained in the model.

A COV effect is deemed significant when the criteria are met and in addition:

- A statistical significant threshold defined as $p<0.05$ ($\chi^2_{p=0.05,\ df=1}=3.84$) for forward selection and as $p<0.01$ ($\chi^2_{p=0.01,\ df=1}=6.63$) for backward elimination is being met.
- Standard error of parameter estimates not larger than 50% of the parameter value and the 95% CI do not include zero.

If applicable, following the above steps, IOV between cycles was modeled as described by Karlsson and Sheiner (1993).

$$P_i = \theta_i \cdot \exp(k_{1i} \cdot \mathrm{CYCL}_1 + k_{2i}\mathrm{CYCL}_2 + k_{3i}\mathrm{CYCL}_3 + k_{4i}\mathrm{CYCL}_4 + \eta_i)$$

where P_i is a PK parameter of the ith individual; θ_i is the mean population estimate; CYCL_1, CYCL_2, CYCL_3 and CYCL_4 are fixed to 1 for the respective cycle and to 0 otherwise; k_{1i}, k_{2i}, k_{3i} and k_{4i} are random variables, representing the shift of P_i from one cycle to another (IOV) and ETA (η_i) represents the shift of P_i from θ_p (inter-patient variability). These random variables are assumed to be symmetrically distributed around 0 with identical variance for k_{1i}, k_{2i}, k_{3i} and k_{4i}, denoted by π^2 and with variance–covariance matrix Ω for ETA (η_i) denoted by diagonal elements ($\omega_1^2, \ldots, \omega_m^2$, m being the number of parameters). Potential sources of IOV might include mechanistic reasons, data collection or study design issues.

The final model contains estimates for the PK parameters and their associated inter-patient variability, estimates of the residual variability as well as COV effects and IOV, if applicable. The possible criteria for accepting the NONMEM model estimation as the final run include the following:

- A ''successful minimization'' statement by the NONMEM program;
- The number of significant digits for the precision of the parameter estimate should preferably be ≥ 3 for all parameters (also a criterion for successful termination);
- Parameter estimates should preferably not be close to a boundary;
- There should preferably be no unacceptable trends in the basic goodness of fit plots;
- The included COVs should be physiologically and clinically relevant.

Sensitivity analysis

As a final step, any individual concentration records or complete patient profiles excluded from the analysis were to be re-introduced to evaluate the impact of these outliers on the final parameter estimates.

Model evaluation

Goodness of fit, as assessed from scatter plots of individual (IPRED) and population (PRED) predicted against observed laromsutine concentrations (OBS), as well as scatter plots of weighted residuals (WRES) against PRED and against TIME, was used at each step of the analysis for model qualification.

The predictive performance of the PK model was evaluated by applying a visual predictive check (Gelman et al., 1996; Yano et al., 2001). For the predictive check, the population parameters and their associated variability obtained from the final model were used to simulate predicted individual profiles. The same population as that on which the analysis was performed was sampled one thousand times for the range of doses and observed sampling times. The obtained 90% prediction interval was superimposed on the observations to evaluate their distribution with respect to the 90% PI for each dose or COV subpopulation. The percentage of observations falling outside the 90% PI interval overall and for selected doses was calculated and any outliers were identified and discussed.

Results

Analysis of data sets

Serial PK plasma samples (up to nine time points per patient pre-dose and over a 4 h period following single dose laromustine infusion) were obtained from 106 patients at 154 dosing occasions: 105 profiles from first dose exposure (cycle 1), 42 from second dose exposure (cycle 2), four from third dose exposure (cycle 3) and three from fourth dose exposure (cycle 4). There was one quantifiable pre-dose concentration (50.6 µg/L, ID 51, cycle 1, study CLI-029, patient no. 3107-010), which was set to missing. All other pre-dose concentrations were BLQ. The complete dataset included 1151 PK assessments at times ranging from 0.083 to 5.917 h post start of the infusion and 154 dosing records. No demographic COVs were missing. Clinical chemistry baseline COV values were missing for the following parameters (% missing): albumin (4%), protein (6%), bilirubin (2%), alkaline phosphatase (4%), ALT (7%), AST (40%) and LDH (8%). From the 106 patients included in the complete dataset, 65 patients had PK assessments following one cycle only (ID 64: cycle 1; ID 69: cycle 2), 36 patients following two cycles (cycles 1 and 2), three patients following three cycles (ID 3 and 43: cycles 1, 2 and 3; ID 22: cycles 1, 2 and 4) and two patients following four cycles (ID 7 and 23). During preliminary analyses treating each dosing occasion as independent, five individual concentration records during the first cycle of treatment, arising from three AML patients (IDs 84, 89, 90) taking part in study CLI-033, were identified as pharmacokinetically inconsistent (high outliers).

In addition, profiles from AML patient IDs 55 and 65 (study CLI-029) in cycle 1 and patient ID 62 (study CLI-029)

in cycle 2 had very high concentrations at serial samples. During preliminary runs it was noted that these profiles interfered with the successful convergence of the minimization procedure and the implementation of the covariance estimation step. The above individual concentration records and all data from patients ID 55 and 65 (cycle 1) were excluded from the analysis. Patient ID 62 cycle 2 profile was also excluded but cycle 1 profile was retained. Thus, the reduced NONMEM analysis dataset included 104 patients, 1122 PK assessments at times ranging from 0.083 to 5.417 h post start of the infusion, and 151 dosing occasions (103 from first dose exposure [cycle 1], 41 from second dose exposure [cycle 2], four from third dose exposure [cycle 3] and three from fourth dose exposure [cycle 4]). Of the 104 patients in the reduced dataset, 64 had PK assessments following one cycle only (ID 63: cycle 1; ID 69: cycle 2), 35 patients following 2 cycles (Cycles 1 and 2), three patients following 3 cycles (IDs 3 and 43: Cycles 1, 2 and 3; ID 22: Cycles 1, 2 and 4) and two patients following 4 cycles (IDs 7 and 23).

PK analysis results

Base model development

One, two and three compartment PK models with zero order input, parameterized in clearance and volume terms (ADVAN1 TRANS2, ADVAN3 TRANS4 and ADVAN11 TRANS4, respectively) were tested and a two compartment model was found to best describe the data. Alternative parameterization in terms of V_{ss} (TRANS3) was also tested but failed to converge successfully. Models utilizing untransformed and log-transformed observations and predictions (laromustine concentration) were tested and using untransformed data resulted in a more even random distribution of the weighted residuals, therefore untransformed concentrations were used thereafter.

The FOCE and INTER estimation methods were tested first. However, problems were encountered with the COV step. Convergence of the minimization procedure was highly dependent on initial estimates and in all subsequent analysis the FO estimation method was applied. The distribution of the parameters, when the FO estimation method was used, resembled the log normal distribution. FO method was used as estimation method.

Initially, the complete dataset was used. Exponential error terms for inter-patient variability on all PK parameters and proportional, additive and combined residual variability models were tested. Since bioanalytical assay variability is confounded in the residual variability estimated by the model, the inclusion of separate residual error terms for each method was also tested. During these steps, PK outliers were identified, the presence of which did not permit estimation of the variability terms with adequate precision. These were excluded from the analysis and the above steps were repeated with the reduced dataset. All subsequent analyses were performed using the reduced dataset.

It was not possible to estimate inter-patient variability on inter-compartmental clearance with adequate precision. Further, despite the lower objective function reached when using a model with a separate residual error term for bioanalytical assay VNPHPP and a common residual error term for assays MET010 and QC-T035, no improvement in terms of inter-patient or residual variability was observed versus the simpler model, and a common residual error term for all assays was considered adequate.

The Base model was a two-compartment PK model estimating total clearance (CL), volume of distribution of the central compartment (V_1), inter-compartmental clearance (Q) and volume of distribution of the peripheral compartment (V_2) (ADVAN3 TRANS4), with exponential error models for inter-patient variability on CL, V_1 and V_2 and a proportional error model for residual variability. The model was fitted to untransformed concentrations using the FO estimation method in NONMEM. The distribution of the parameters when the FO estimation method was used resembled the log normal distribution.

The estimation and COV routines converged successfully and precision in both structural and variance parameter estimates was good. Goodness of fit (GoF) plots of observed (DV) versus predicted laromustine concentrations (population [PRED] and individual [IPRED]) and weighted residuals (WRES) versus TIME and versus PRED plots are plotted. No bias was observed in the DV versus PRED and IPRED plots and there was good agreement between predictions and observations. No trends were observed in the WRES versus TIME plots and randomness was observed in the WRES versus PRED plots. The Base model provided individual empirical Bayesian PK parameter estimates common for all dosing occasions of a given subject by evoking the POSTHOC option in NONMEM, and was used for COV evaluation in conjunction with cycle baseline COV values.

Covariate analysis

Scatterplots of individual empirical Bayes estimates of ETA CL, ETA V_1 and ETA V_2 from the Base model against Dose, BSA, age, body weight, creatinine clearance, and actual levels of serum creatinine, albumin, total proteins, bilirubin, alkaline phosphatase, ALT, AST and LDH were constructed. In addition, box plots of individual empirical Bayes estimates of ETA CL, ETA V_1 and ETA V_2 from the Base model were constructed by phase, cycle, gender, ethnic origin, tumor type and categories (within, above and below normal limits and missing values) for serum creatinine, albumin, total proteins, bilirubin, alkaline phosphatase, ALT, AST, and LDH.

Despite the fact that no obvious relationships were observed from close examination of the plots, the COV evaluation steps were performed in NONMEM for completeness. AST was not evaluated as a COV, since information in this parameter was missing in more than 30% of the subjects. The remaining clinical chemistry parameters were evaluated as CCOVs.

During the single COV analysis, when COVs were introduced into the model one at a time, COV effects were selected for inclusion in the forward selection step if they resulted in a statistically significant reduction of the OFV and model parameters were estimated with adequate precision (95% CI did not include zero). Due to the high correlation between BSA and body weight, when both COVs were identified as significant only BSA was selected, since this class of drugs are commonly dosed based on BSA.

The COV effect that resulted in the greater reduction of the OFV from the single COV analysis was considered the Base1 model for the forward selection step. In this step, the rest of the selected COV effects were introduced into the model in the order of their significance and were only retained if they resulted in a statistically significant reduction of the OFV and model parameters were estimated with adequate precision (95% CI did not include zero).

The model with the effect of tumor type on CL, LDH and serum creatinine on V_2 and age on V_1 comprised the most complex model and was considered the Base2 model for the backward elimination step. During that step, when COV effects were removed one at a time, in the reverse order of their significance, all the above effects caused a significant increase in the OFV; therefore, they were retained in the model.

Inter-occasion variability and model refinement

When examining individual observed and predicted concentrations versus time plots from the Base2 model, despite the inclusion of COVs, some lack of fit was still observed in profiles from patients that had received more than one cycle, indicating that inclusion of IOV should be considered. In addition, when inter-patient and residual variability estimates from Base2 model are compared to those of the Base model, no improvement is observed, indicating that no portion of the variability was explained by the inclusion of the selected COV effects. This was consistent with the lack of trends observed in the ETAs versus COV plots from the Base model.

In the next step, IOV was introduced in the Base2 model, to account for deviations in PK parameters between cycles and to further evaluate the significance of the identified COV effects. Various combinations of IOV variability terms were assigned to CL, V_1 and V_2, and models were tested allowing IOV either to differ for each parameter or to be the same. Despite the fact that including IOV in the Base2 model resulted in a marked drop in the NONMEM OFV, parameters and inter-patient error terms were not reliably estimated.

Given obvious differences between cycles in the observed profiles from patients that had received more than one cycle and since none of the identified COVs appear to explain part of the inter-patient variability, Base2 model was considered over-parameterized and it was deemed appropriate to revert to the Base model with no COV effects. Inclusion of various combinations of IOV terms was tested and all resulted in marked reductions in the OFV. The model with IOV terms on CL and V_1 resulted in reliable parameter estimates, as well as a reduction in inter-patient and residual variability. Seeking further improvement in variability estimates, the FOCE and INTER estimation methods were employed, however errors were issued from the estimation step and the COV step was either not implemented or aborted.

Final model

The final population PK model for laromustine was a two-compartment PK model with zero order input, parameterized in terms of total clearance (CL), volume of distribution of the central compartment (V_1), inter-compartmental clearance (Q) and volume of distribution of the peripheral compartment (V_2), with exponential error models for inter-patient variability on CL, V_1 and V_2, IOV on CL and V_1 and a proportional error model for residual variability. The model was fitted to the untransformed data using the FO estimation method, the estimation and COV routines converged successfully with structural, inter-patient and residual variability parameters estimated with good precision.

Goodness of fit (GoF) plots of observed (OBS) versus predicted laromustine concentrations (population [PRED], and individual [IPRED]) and weighted residuals (WRES) versus TIME and versus PRED for the final model are presented in Figure 2. No bias was observed in the OBS versus PRED and IPRED plots and there was very good agreement between predictions and observations. No trends were observed in the WRES versus TIME plots and there was randomness in the WRES versus PRED plots. Histograms of empirical Bayesian estimates of the parameters for the final model were presented. No significant trends were observed in box-plots and scatter-plots of empirical Bayesian estimates of laromustine PK parameters from the final model against COVs. Specifically, box-plots of estimated and derived PK parameters by Cycle show no differences in laromustine PK parameters between the first and subsequent cycles ($n = 103$, 41, 4 and 3 for Cycles 1,2, 3 and 4, respectively), suggesting time-linearity in laromustine pharmacokinetics. The lack of trends in scatterplots of estimated and derived PK parameters against dose, suggests dose-linearity in laromustine pharmacokinetics across a broad dose range (3–708 mg/m^2).

The population parameter estimates from the final model are presented in Table 2. Laromustine total clearance and volume of distribution of the central compartment were 96.3 L/h and 45.9 L, with inter-patient variability of 52.9% and 79.8%, respectively. This variability could not be explained by any of the tested COVs, while IOV was 26.7% and 49.3% for CL and V_1, respectively. The population estimates for Q and V_2 were 73.2 L/h and 29.9 L, respectively, and inter-patient variability in V_2 was 63.1%. Structural parameter estimates were similar to those for the Base model while inter-patient variability in CL and V_1, although slightly reduced, still remained high. Residual variability dropped from 36.3% for the Base model to 29.7% for the Final model. Summaries of empirical Bayesian and derived PK parameters for the final model, overall and for Cycles 1 and 2 show no differences in PK parameters between cycles.

Sensitivity analysis

The final model was applied to the complete NONMEM dataset, and while estimation and covariance steps converged successfully, inter-patient variability parameters were not estimated with good precision (%RSE 47–110%). Laromustine population PK parameters were estimated from the final model run including outliers. Differences from the run with the reduced dataset in structural parameter estimates were observed, mainly in Q and V_2, which 80 and 40% reduced, respectively. Inter-patient variability estimates were inflated by 65–90%, IOV estimates by 130–160% and residual variability by 44% relatively to the run with the reduced dataset.

The results of this analysis supported the decision to exclude a small percent (3%) of the observations that would

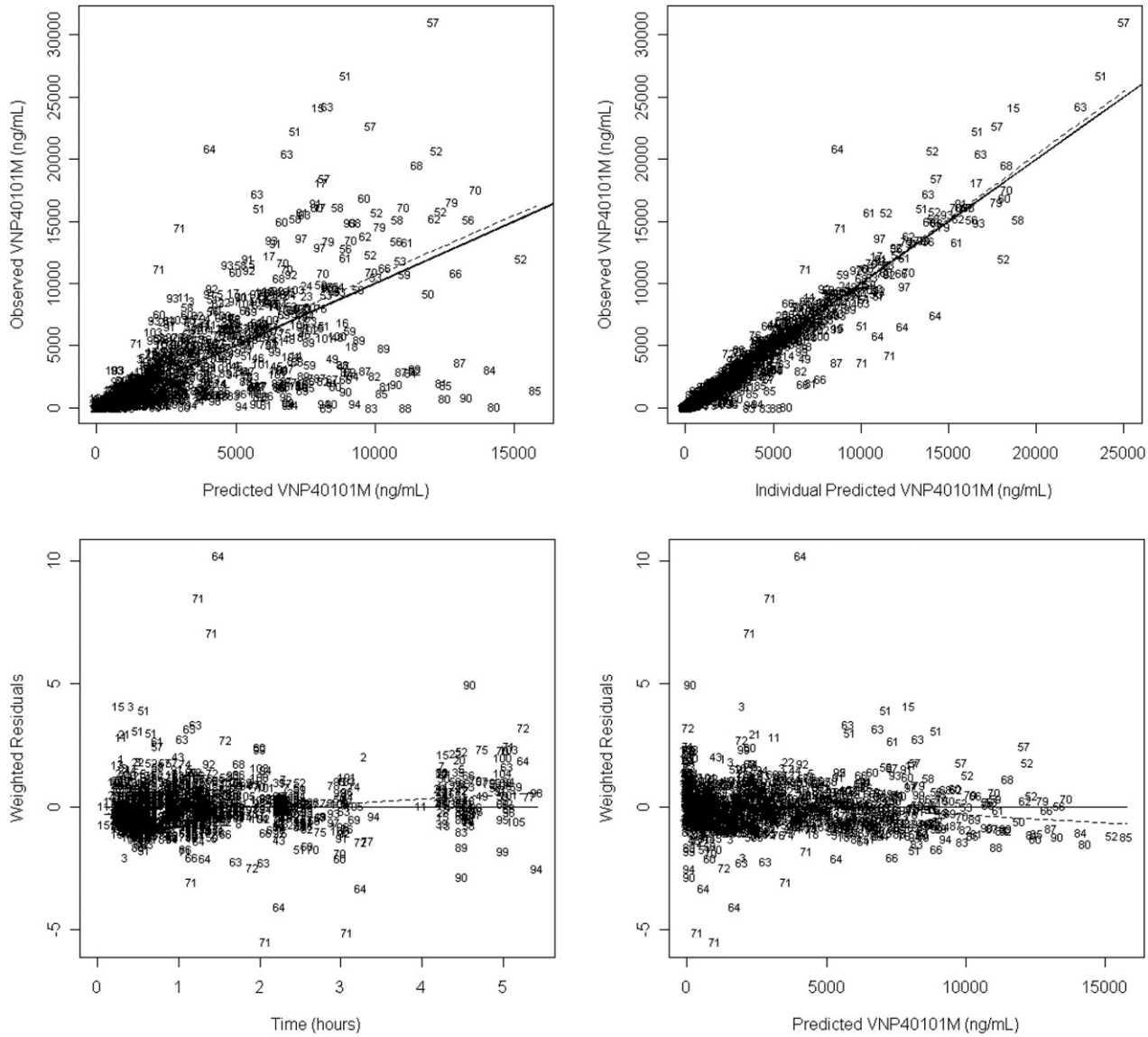

Figure 2. Final model GoF plots: DV versus PRED and IPRED with line of identity and WRES versus TIME and versus PRED with regression line.

Table 2. Laromustine population PK parameter estimates from the final model.

Model parameter	Estimate [95% CI]	(%RSE)[a]
CL (L/h)	96.3 [82.7–110]	7.23
V_1 (L)	45.9 [31.3–60.5]	16.3
Q (L/h)	73.2 [39.7–107]	23.4
V_2 (L)	29.9 [22.4–37.4]	12.8
Inter-patient variability in CL (%CV)[b]	52.9	20.3
Inter-patient variability in V_1 (%CV)[b]	79.8	27.0
Inter-patient variability in V_2 (%CV)[b]	63.1	35.4
Inter-occasion variability in CL[b]	26.7	26.7
Inter-occasion variability in V_1[b]	49.3	69.5
Proportional residual variability (%CV)[b]	29.7	43.6

[a]%RSE was calculated as the S.E. divided by the parameter estimate × 100.

[b]The %CV for both inter-patient and residual variability is taken as the square root of the variance × 100.

have had such a large effect on structural and variability parameter estimates. The reason for the three outlying profiles belonging to patient IDs 55, 65 (cycle 1) and 62 (cycle 2) could not be attributed to any of the available COV information as these patients did not share any abnormalities in terms of demographics or organ function.

Model evaluation

Examination of the goodness of fit plots show no bias and very good agreement between predictions and observations, as well as lack of trends and randomness in the residual plots (Figure 2), thus confirming the validity of the model. Visual predictive checks were performed using the Final model for each dose level. Predicted and observed concentrations were grouped by nominal time after the end of the infusion and the % observations outside the respective 90% CI were calculated for each dose level and overall.

The 90% PIs simulated by dose, with observations superimposed, for all dose levels are determined. Overall

and for each dose level, the majority of the observations was included in the 90% PI. The 90% PIs simulated by cycle, with observations superimposed for doses 100 mg/m^2 (representing 8.6% of the total observations included in the analysis) and 600 mg/m^2 (28.2% of the total observations included in the analysis) for Cycles 1, 2 and overall are presented in Figures 3 and 4, respectively. These plots confirm the validity of the Final model that assumes the pharmacokinetics of laromustine are independent of dose for the range studied and that any differences in patient profiles between cycles are accounted for by IOV.

Discussion

Considerable variability was associated with the laromustine concentration–time profiles, mainly between patients but also between cycles for the same patient, for all doses. This had been observed during NCA PK analysis of the individual studies. In general, laromustine concentrations appear to decline bi-exponentially following termination of the IV infusion; although, for individual cases associated with the lower doses only, a mono-exponential phase could only be observed. When tested, a two-compartment model was clearly superior to a one-compartment model. A three compartment model was also tested but did not converge successfully. First-order conditional and first-order conditional with interactions estimation methods were tested but there were problems with the minimization routine and implementation of the covariance step, therefore the FO method was used throughout. The models were fitted to both untransformed and log-transformed data, however trends were observed in the residual lots when log transformation was used, thus it was decided to proceed with untransformed data.

The population PK model for laromustine was thus a two-compartment PK model parameterized in terms of total clearance (CL), volume of distribution of the central compartment (V_1), inter-compartmental clearance (Q), and volume of distribution of the peripheral compartment (V_2). Exponential error terms were evaluated for inter-patient variability on all structural parameters; however, the term for inter-compartmental clearance (Q) had to be set to zero. Since bioanalytical assay variability is confounded in the residual variability estimated by the model, the inclusion of separate residual error terms for each of the three methods used was also tested but a proportional error model common for all assay methods was found to adequately describe residual variability (representing a composite of model misspecification, assay variability and intra-patient variability).

Demographics (BSA, age, weight, gender and ethnic origin), as well as study Phase, tumor type, dose, and cycle were tested as COVs. Kidney function, as assessed by creatinine clearance, and liver function, as assessed by albumin, total proteins, bilirubin, alkaline phosphatase, ALT and LDH, were also tested. Overall, COV values were quite similar between the first and subsequent cycles, apart from LDH, due to a couple of very high values observed in the first cycle. When plots of individual Bayes empirical estimates of the PK and inter-patient variance parameters from the Base model were examined, no obvious relationships were observed, nevertheless, the full COV evaluation was performed in NONMEM for completion.

Although during the formal COV evaluation a number of effects (Tumor type on CL, LDH and serum creatinine on V_2 and age on V_1) were identified as statistically significant, their inclusion did not appear to explain any portion of the inter-patient variability in PK parameters, or reduce residual variability. In addition, when IOV was introduced in the model that included COVs, in order to account for differences observed between cycles in individual profiles arising from the same patients, PK parameters and their variability could not be reliably estimated.

Based on the above evaluation it was deemed appropriate to revert to the Base model without COVs, to which IOV was included as an additive term on the variance of CL and V_1 and resulted in a reduction of the residual variability. This was then considered the final population PK model. The population estimates for laromustine total clearance and volume of distribution of the central compartment were 96.3 L/h and 45.9 L, associated with high inter-patient variability of 52.9% and 79.8%, respectively, and IOV 26.7% and 49.3%, respectively. The population estimates for Q and V_2 were 73.2 L/h and 29.9 L, respectively, and inter-patient variability in V_2 was 63.1%. Residual variability was 29.7%.

Following preliminary evaluations, a limited number of individual concentrations and three complete patient profiles were excluded from the analysis since it was thought that they might obscure any potential COV relationships. When these were re-introduced and the Final model was applied to the complete dataset, differences in structural parameters Q and V_2 were observed. The estimates of variability parameters appeared to be inflated and were also not reliably estimated. These results supported the decision to exclude a small percent (3%) of the observations that would have had such a large effect on structural and variability parameter estimates. The reason for the three outlying profiles belonging to patient IDs 55, 65 (cycle 1) and 62 (cycle 2) could not be attributed to any of the available COV information as these patients did not share any abnormalities in terms of demographics or organ function.

The final model was further evaluated using visual predictive checks by dose and 93% of the total observations were included within the 90% PI. For the 100 and 600 mg/m^2 dose, which represent 8.6 and 28.3% of the observations, respectively, at least 89.5% of the observations for each cycle were included within the 90% PI. This confirmed the validity of the Final model that assumes the pharmacokinetics of laromustine are independent of dose for the range studied and that any differences in patient profiles between cycles are accounted for IOV.

Mean NCA analysis estimates of CL and V_{ss} from studies CLI-011 and CL-029, were 95.0 L/h and 60.4 L and 103.1 L/h and 89.6 L, respectively, with coefficient of variation, %CV, ranging from 39 to 74%. Mean NCA analysis estimates of CL and V_{ss} from studies CLI-028, CLI-033 and CLI-043 ranged from 261 to 352 L/h and 206 to 370 L, respectively, with %CV ranging from 70 to 203%. Mean NCA terminal half-life estimates for all five studies ranged from 0.673 to 0.841 h, with a % CV of 18 to 34%.

The population estimate for laromsutine clearance, derived V_{ss} and $t_{1/2}\beta$ (96.3 L/h, 75.8 L and 0.684 h respectively) are

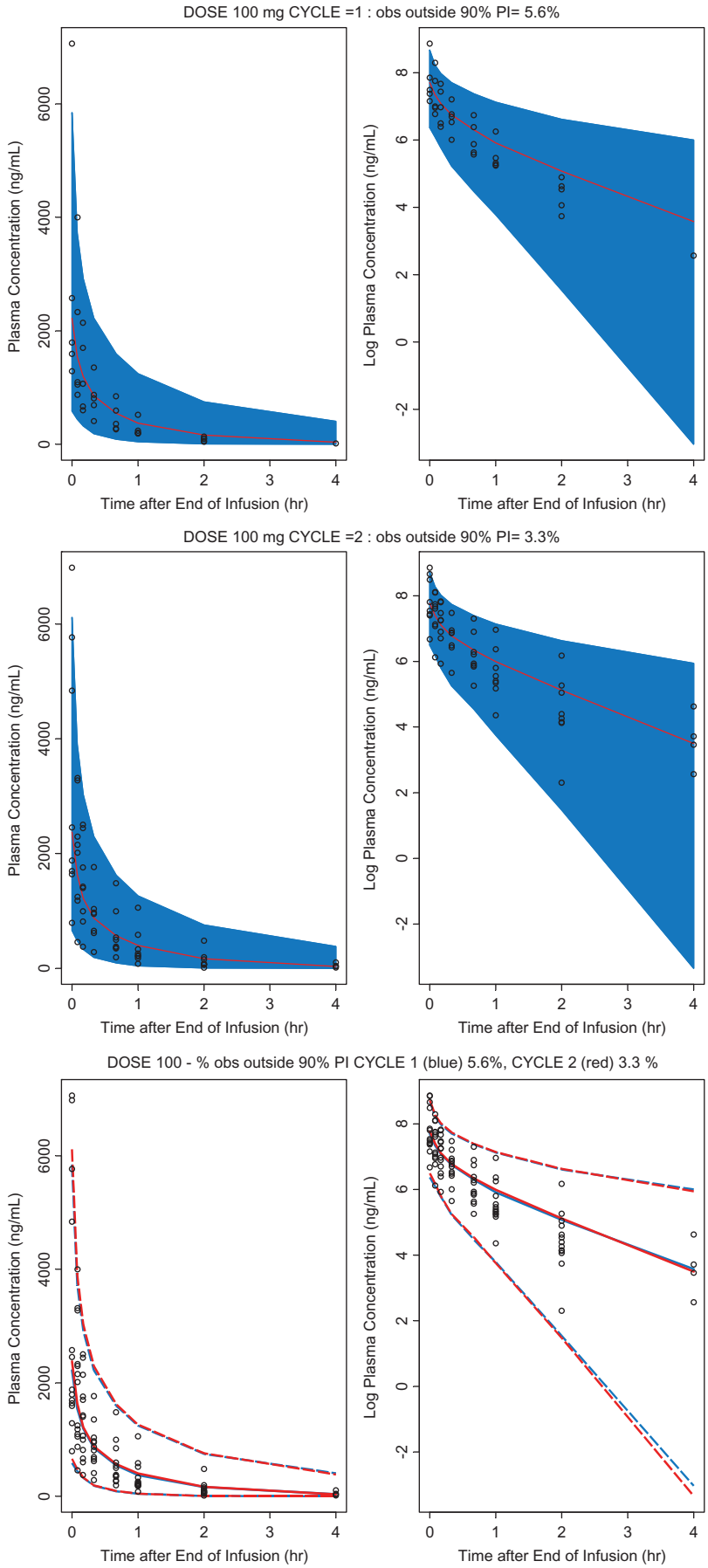

Figure 3. Dose 100 mg/m^2: visual predictive check for final PK model.

DOI: 10.1080/00498254.2016.1201703

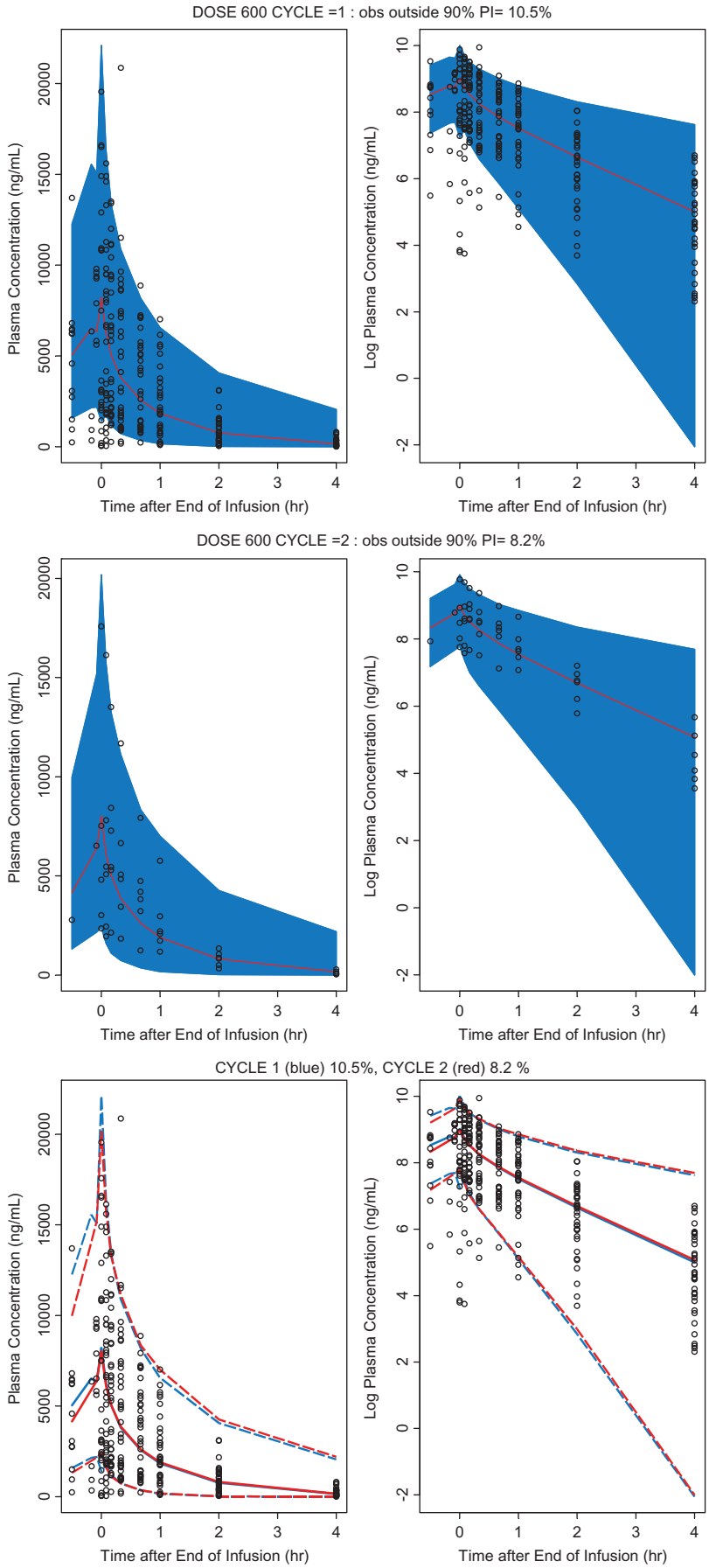

Figure 4. Dose 600 mg/m^2 by cycle: visual predictive check for final PK model.

similar to those from studies CLI-011 and CL-029, which account for about 60% of the profiles (55% of the patients) included in the analysis. This estimate of systemic clearance is equal to or greater than the human liver blood flow rate (87 L/h) and V_{ss} is double that of total body water (42 L), indicating that laromustine is distributed to tissues. The very high systemic clearance is consistent with extra-hepatic elimination, with rapid, non-enzymatic degradation, also a plausible mechanism.

Conclusions

A two-compartment PK model parameterized in terms of total clearance (CL), volume of distribution of the central compartment (V_1), inter-compartmental clearance (Q) and volume of distribution of the peripheral compartment (V_2), with exponential error models for inter-patient variability, a proportional error model residual variability and IOV on CL and V_1 adequately described the concentration–time profiles following laromustine infusion. The population estimates for laromustine CL and V_1 were 96.3 L/h and 45.9 L and were associated with high inter-patient variability of 52.9% and 79.8% and IOV of 26.7% and 49.3% for CL and V_1, respectively. The population estimates for laromustine Q and V_2 were 73.2 L/h and 29.9 L, respectively, and inter-patient variability in V_2 was 63.1%. COVs including demographics, dose, cycle, type of tumor, renal function and liver function did not explain any of the variability in laromustine PK parameters. Visual predictive checks using the final model showed that the majority (93.3%) of the observed laromsutine concentrations were within the 90% prediction intervals. The population estimate of systemic clearance is equal to or greater than the human liver blood flow rate, consistent with extra-hepatic elimination or degradation. The estimated V_{ss} (75.8 L) exceeds total body water, indicating that laromsutine is distributed to tissues. The half-life is short, less than 1 h, reflecting the rapid clearance. Population PK analysis showed laromustine pharmacokinetics to be independent of dose and organ function with no effect of subsequent dosing cycles, although considerable inter-patient and IOV was observed.

Acknowledgements

These studies were done at ICON Development Solutions, Skelton House, Manchester Science Park, Lloyd Street North, Manchester M15 6SH, UK for Vion Pharmaceuticals Inc. We would like to thank Drs. Maria Pitsiu and Ziad Hussein of ICON, Miganush Stepanians and Nicole LaVallee of PROMETRIKA for performing and supervising these studies. We would like to thank Ray F. Nassar for helping in the editing process.

In Memoriam to Dr. Alan C. Sartorelli. Alan C. Sartorelli, Ph.D. was a professor of pharmacology for over 50 years at Yale School of Medicine, director of the Yale Comprehensive Cancer Center and chair of the Department of Pharmacology. His career highlights include receiving the Yale Comprehensive Cancer Center Lifetime Achievement Award in 2011, the Otto Krayer Award in Pharmacology in 2002, the Experimental Therapeutics Award from the American Society of Pharmacology and Experimental Therapeutics, also in 2002, the Bruce F. Cain Memorial Award in 2001, and the Mike Hogg Award from the UTMD Anderson Cancer Center in 1989. Dr. Sartorelli authored and coauthored over 700 papers published in various scientific journals, and was the founding editor of *Pharmacology and Therapeutics*, and co-inventor on 16 U.S. patents for anti-cancer therapy. Laromustine is one of the compounds which was invented in his laboratory and has entered into advanced clinical trials.

Declaration of interest

We declare no financial conflict of interest.

References

Abdelhameed M. (2008). Pharmacokinetics of cloretazine (VNP40101M) and its metabolite VNP4090CE in human plasma samples from clinical study CLI-043. Vion Report CLI-043b (Covance Report 7660-122).

Davies B, Morris T. (1993). Physiological parameters in laboratory animals and humans. Pharm Res 10:1093–5.

Finch RA, Shyam K, Penketh PG, Sartorelli AC. (2001). 1,2-Bis(methylsulfonyl)-1-(2-chloroethyl)-2-(methylamino)carbonylhydrazine (101M): a novel sulfonylhydrazine prodrug with broad-spectrum antineoplastic activity. Cancer Res 61:3033–8.

Gelman A, Bios A, Jiang J. (1996). Physiological pharmacokinetic analysis using population modelling and informative prior distribution. J Am Stat Assoc 91:1400–12.

Guidance for Industry. (1999). Population pharmacokinetics. U.S. Food and Drug Administration.

Guideline on reporting. (2007). The results of the population pharmacokinetic analyses. European Medicines Agency.

Jiang X. (2008). Pharmacokinetic report for a phase II study of VNP40101M for patients with acute myelogenous leukemia or high-risk myelodysplasia. Vion Report CLI-033b (Covance Report 7660-123).

Karlsson MO, Sheiner LB. (1993). The importance of modelling inter-occasion variability in population pharmacokinetic analyses. J Pharmacokinet Biopharm 21:735–50.

Meister A, Anderson ME. (1983). Glutathione. Annu Rev Biochem 52: 711–60.

Moriarty-Craige SE, Jones DP. (2004). Extracellular thiols and thiol/disulfide redox in metabolism. Annu Rev Nutr 24:481–509.

Nassar A. (2008a). Pharmacokinetics of VNP40101M and VNP4090CE in cancer patients from Vion Clinical Study CLI-011. Vion Report CLI-011a.

Nassar A. (2008b). Pharmacokinetics of VNP40101M and VNP4090CE in cancer patients from Vion Clinical Study CLI-028. Vion Report CLI-028a.

Nassar A. (2008c). Pharmacokinetics of VNP40101M and VNP4090CE in cancer patients from Vion Clinical Study CLI-029. Vion Report CLI-029a.

Nassar AE, King I, Paris BL, et al. (2009). An in vitro evaluation of the victim and perpetrator potential of the anti-cancer agent laromustine (VNP40101M), based on reaction phenotyping and inhibition and induction of cytochrome P450 (CYP) enzymes. Drug Metab Dispos 37:1922–30.

Nassar AE, Du J, Belcourt M, et al. (2010a). Chapter 6, ''Biotransformation and metabolite elucidation of xenobiotics''. In: Nassar A-EF, ed. Case study: identification of in vitro metabolite/decomposition products of the novel DNA alkylating agent laromustine. Hoboken, NJ: John Wiley & Sons.

Nassar AE, Du J, Belcourt M, et al. (2010b). Chapter 5, ''Biotransformation and metabolite elucidation of xenobiotics''. In: Nassar A-EF, ed. Case study: the unanticipated loss of N2 from novel DNA alkylating agent laromustine by collision-induced dissociation: novel rearrangements. Hoboken, NJ: John Wiley & Sons.

Nassar AE, King I, Du J. (2010c). In vitro profiling and mass balance of the anti-cancer agent laromustine [^{14}C]-VNP40101M by rat, dog, monkey and human liver microsomes. Open Drug Metab J 4:1–9.

Nassar AE, King I, Du J. (2011). Characterization of short-lived electrophilic metabolites of the anticancer agent laromustine (VNP40101M). Chem Res Toxicol 24:568–78.

Nassar AF, Wisnewski A, King I. (2015). Metabolic disposition of the anti-cancer agent [(14)C]laromustine in male rats. Xenobiotica 45:711–21.

Penketh PG, Shyam K, Sartorelli AC. (1994). Studies on the mechanism of decomposition and structural factors affecting the aqueous stability of 1,2-bis(sulfonyl)-1-alkylhydrazines. J Med Chem 37:2912–7.

Penketh PG, Shyam K, Sartorelli AC. (2000). Comparison of DNA lesions produced by tumor-inhibitory 1,2-bis(sulfonyl)hydrazines and chloroethylnitrosoureas. Biochem Pharmacol 59:283–91.

Piotmovsky VR. (2000). Population pharmacodynamic and pharmacokinetic modelling via mixed effects. Curr Opin Drug Discov Dev 3: 314–30.

Pratviel G, Shyam K, Sartorelli AC. (1989). Cytotoxic and DNA-damaging effects of 1,2-bis(sulfonyl)hydrazines on human cells of the Mer + and Mer − phenotype. Cancer Biochem Biophys 10:365–75.

Shyam K, Cosby LA, Sartorelli AC. (1985). Synthesis and evaluation of N,N′-bis(arylsulfonyl)hydrazines as antineoplastic agents. J Med Chem 28:525–7.

Shyam K, Furubayashi R, Hrubiec RT, et al. (1986). 1,2-bis(arylsulfonyl)hydrazines. 2. The influence of arylsulfonyl and aralkylsulfonyl substituents on antitumor and alkylating activity. J Med Chem 29:1323–5.

Shyam K, Hrubiec RT, Furubayashi R, et al. (1987). 1,2-Bis(sulfonyl)hydrazines. 3. Effects of structural modification on antineoplastic activity. J Med Chem 30:2157–61.

Shyam K, Penketh PG, Divo AA, et al. (1993). Synthesis and evaluation of 1-acyl-1,2-bis(methylsulfonyl)-2-(2-chloroethyl)hydrazines as antineoplastic agents. J Med Chem 36: 3496–502.

Shyam K, Penketh PG, Loomis RH, et al. (1996). Antitumor 2-(aminocarbonyl)-1,2-bis(methylsulfonyl)-1-(2-chloroethyl)-hydrazines. J Med Chem 39:796–801.

Yano Y, Beal SL, Sheiner LB. (2001). Evaluating pharmacokinetic/pharmacodynamic models using the posterior predictive check. J Pharmacokinet Pharmacodyn 28:171–92.

Supplementary material available online

Please see Tables 1–8 and Figures 1–4 in the supplementary file for more details about the methods and data used in the manuscript.